Inhalation of methane preserves the epithelial barrier during ischemia and reperfusion in the rat small intestine

András T. Mészáros, MD, Tamás Büki, MD, Borbála Fazekas, MD, Eszter Tuboly, PhD, Kitti Horváth, MD, Marietta Z. Poles, PhD, Szilárd Szűcs, MD, Gabriella Varga, PhD, József Kaszaki, PhD, *and* **Mihály Boros, MD, PhD, DSc,** *Szeged, Hungary*

Background. *Methane is part of the gaseous environment of the intestinal lumen. The purpose of this study was to elucidate the bioactivity of exogenous methane on the intestinal barrier function in an antigen-independent model of acute inflammation.*
Methods. *Anesthetized rats underwent sham operation or 45-min occlusion of the superior mesenteric artery. A normoxic methane (2.2%)-air mixture was inhaled for 15 min at the end of ischemia and at the beginning of a 60-min or 180-min reperfusion. The integrity of the epithelial barrier of the ileum was assessed by determining the lumen-to-blood clearance of fluorescent dextran, while microvascular permeability changes were detected by the Evans blue technique. Tissue levels of superoxide, nitrotyrosine, myeloperoxidase, and endothelin-1 were measured, the superficial mucosal damage was visualized and quantified, and the serosal microcirculation and mesenteric flow was recorded. Erythrocyte deformability and aggregation were tested in vitro.*
Results. *Reperfusion significantly increased epithelial permeability, worsened macro- and microcirculation, increased the production of proinflammatory mediators, and resulted in a rapid loss of the epithelium. Exogenous normoxic methane inhalation maintained the superficial mucosal structure, decreased epithelial permeability, and improved local microcirculation, with a decrease in reactive oxygen and nitrogen species generation. Both the deformability and aggregation of erythrocytes improved with incubation of methane.*
Conclusion. *Normoxic methane decreases the signs of oxidative and nitrosative stress, improves tissue microcirculation, and thus appears to modulate the ischemia-reperfusion–induced epithelial permeability changes. These findings suggest that the administration of exogenous methane may be a useful strategy for maintaining the integrity of the mucosa sustaining an oxido-reductive attack. (Surgery 2017;161:1696-709.)*

From the University of Szeged, Institute of Surgical Research, Szeged, Hungary

Acute mesenteric ischemia progresses rapidly and leads to irreversible damage of the mucosa, but reperfusion can cause injury in excess of that induced by ischemia alone.[1] It is commonly accepted that re-established circulation is associated with the production of reactive oxygen and nitrogen species (ROS and RNS, respectively), which leads subsequently to membrane breakdown and loss of cellular integrity. In this way, events during intestinal ischemia-reperfusion (IR) increase quickly the mucosal permeability which leads to excessive fluid losses and an influx of luminal foreign material into the lamina propria.[2]

It is also recognized that the gastrointestinal (GI) lumen contains a range of potentially bioactive gas metabolites, such as carbon dioxide,[3] hydrogen,[4] ammonia,[5] and hydrogen sulfide.[6]

Supported by grants of the Hungarian Science Research Fund, OTKA K104656, and the National Research Development and Innovation Office, NKFI K120232, NFKI 116861, and GINOP-2.3.2-15-2016-00015.

The authors hereby declare that they had no conflict of interest when carrying out the experiment.

Accepted for publication December 29, 2016.

Reprint requests: Mihály Boros, MD, PhD, DSc, Institute of Surgical Research, University of Szeged, Szőkefalvi-Nagy Béla u. 6, Szeged H-6720, Hungary. E-mail: boros.mihaly@med.u-szeged.hu.

0039-6060/$ - see front matter

http://dx.doi.org/10.1016/j.surg.2016.12.040

Methane (CH_4) is also present in the intestinal atmosphere and is measurable in the exhaled breath of approximately one-third of humans.[7] The functional consequences of CH_4 production are subject to debate; nevertheless, the formation of CH_4 in mammals is regarded as a specific indicator of carbohydrate fermentation by the anaerobe intestinal flora. This latter route dependent on anaerobic flora is probably not exclusive; various in vitro and in vivo experiments have demonstrated alternative routes for the nonbacterial generation of CH_4 in conditions of oxido-reductive stress.[8,9]

Although some data suggest a role in the regulation of GI motility,[10] the in vivo biologic effects of biotic or abiotic CH_4 formation in the gut are still not completely understood. A normoxic CH_4-air mixture decreases the biochemical signs of inflammation after an IR challenge,[11] and a number of other observations confirm the anti-inflammatory properties of CH_4, demonstrated by decreases in levels of inflammatory cytokine and markers of oxidative stress.[12-16] In addition, many published articles suggest that CH_4-based treatments have antiapoptotic effects in model experiments.[17-23]

These converging research findings suggest that CH_4 can influence the permeability status of the mucosa, a most critical factor in GI injuries in clinical settings. Consequently, we devised experiments to investigate the kinetics of CH_4 distribution in the blood and small intestine and the effects of exogenous CH_4 which leads to an approximately twofold increase in the intraluminal CH_4 concentration over background levels; we evaluated these effects on the epithelial and endothelial permeability and secondary inflammatory reactions in a standardized rat model of mesenteric IR.

Because the mucosal response may take the form of either the rapid exacerbation of an injury after the ischemic episode or of a slowly developing alteration,[24] another goal of the study was to characterize the consequences of normoxic CH_4 inhalation separately in an early and a late period of an IR-induced, antigen-independent inflammatory challenge. Finally, additional in vitro model experiments were performed to test the influence of CH_4 on erythrocyte membrane rigidity to investigate possible mechanisms of changes in the microcirculation of the small intestine.

MATERIALS AND METHODS

The experiments were carried out on 76, male, Sprague-Dawley rats (280–320 g body weight [bw]) in accordance with the National Institutes of Health guidelines on the handling and care of experimental animals and the EU Directive 2010/63 for the protection of animals used for scientific purposes; the study was approved by the National Scientific Ethical Committee on Animal Experimentation (National Competent Authority), with license number V/148/2013. The animals were housed in plastic cages in a 12/12-h day/night cycle under standard air temperature and humidity conditions. All chemicals were obtained from Sigma-Aldrich Inc (Budapest, Hungary) unless stated otherwise.

Operative procedure. Rats fed on a normal laboratory diet with tap water ad libitum were allocated randomly into one or the other of the experimental groups. After overnight fasting, the animals were anesthetized with sodium pentobarbital (50 mg/kg bw intraperitoneal) and placed in a supine position on a heating pad. The trachea was dissected free and cannulated with a silicone tube; then the right jugular vein was cannulated with PE50 tubing for fluid administration and Ringer's lactate infusion (10 mL/kg/h) during the experiments.

Experimental protocol. The experiments were performed in 2 series (Fig 1). In study 1 (the "early reperfusion" study), the animals were killed 60 min after the re-establishment of the mesenteric blood flow; in the second set (the "late reperfusion" study), the reperfusion period and the corresponding control phase in the sham-operated animals lasted for 180 min.

After a midline laparotomy, the superior mesenteric artery (SMA) was dissected free. Group 1 ($n = 6$) served as a sham-operated control, while in Group 2 (IR, $n = 6$), the SMA was occluded using an atraumatic vascular clip for 45 min. In the CH_4-treated Group 3 (IR + CH_4, $n = 6$) an artificial gas mixture containing 2.2% CH_4, 21% O_2, and 76.8% N_2 (Linde Gas, Budapest, Hungary) was administered for 5 min before the end of the 45-min ischemia and for 10 min at the beginning of the reperfusion (Fig 1). In study 2, the protocol followed was identical, but the durations of the observation and the reperfusion phases were different.

Epithelial permeability. Epithelial permeability was determined with the 4 kDa fluorescein isothiocyanate-dextran (FD4) method, as described previously.[25] In short, a 5-cm-long segment of the terminal ileum supplied by 3 blood vessel arcades was isolated at a distance of 10 cm from the ileocecal valve. Silicone cannulas were placed and fixed into the oral and aboral ends of the segment, and the lumen was gently flushed with 5 mL of 37°C

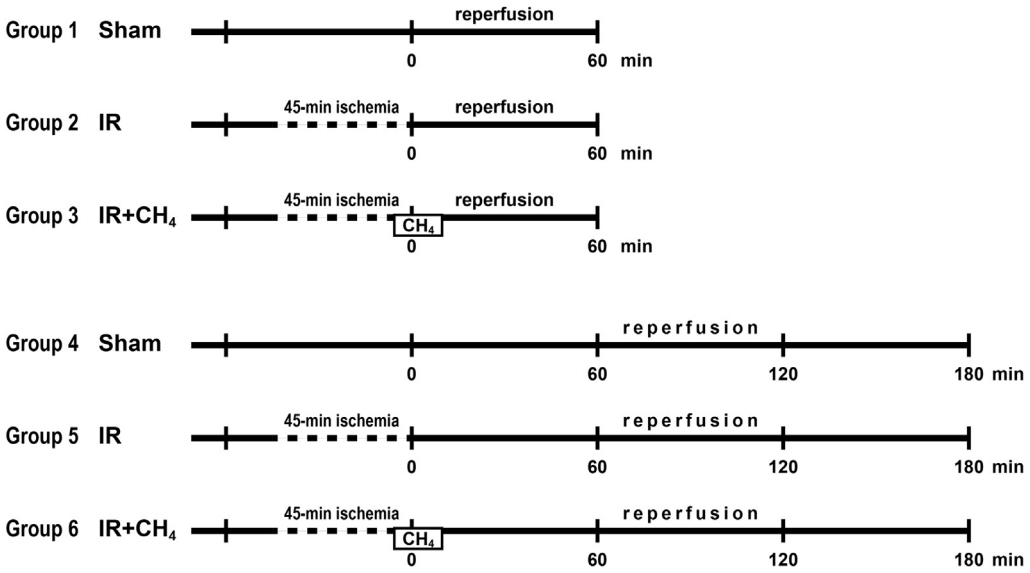

Fig 1. The experimental scheme. Rats were assigned randomly to 3 groups and each experimental group was divided into 2 subgroups to simultaneously allow the assessment of permeability and structural changes in the early and late reperfusion phases.

154 mM NaCl and 5 mL air; then the distal end was closed.

Before performing measurements, the renal pedicles were ligated. Exactly at the moment of reperfusion (the "early reperfusion" study) or 120 min later (the "late reperfusion" study), the lumen was filled with 0.5 mL of warmed (37°C) FD4 solution (25 mg/mL). Blood samples (0.3 mL) were then taken 5, 10, 20, 30, and 40 min later for measurement of plasma fluorescein concentration with a fluorescence spectrophotometer (F-2000; Hitachi, Tokyo, Japan, Ex: 492 nm; Em: 515 nm). The blood samples were stored on ice in the dark and centrifuged at 100*g* for 10 min. At the end of the experiment, the bowel segment was removed and weighed. The epithelial permeability index was expressed as a percentage of FD4 measured in the plasma calculated using the formula (arterial FD4 concentration [ng/mL]/luminal FD4 concentration [ng/mL] * 100).

Intestinal vascular permeability. The vascular permeability index was determined using the azo dye Evans blue method, as described previously.[26] In brief, 30 min before the end of the experiments, 20 mg/mL/kg of Evans blue was given in intravenous bolus and, at the end of the experiments, a blood sample was taken from the caval vein together with a whole-thickness tissue sample from the ileum. The biopsy specimen was placed in 5 mL of formamide and homogenized for 1 min in a glass Potter homogenizer. The homogenate was incubated at room temperature for 20 h and then centrifuged at 2500*g* for 30 min.

The absorbance of the supernatant was determined at 650 nm with a UV-1601 spectrophotometer (Shimadzu Corp, Kyoto, Japan) against a formamide blank. The concentration of Evans blue was determined from a standard curve and was normalized to the protein content of the samples.[27] Similarly, blood samples were centrifuged at 600*g* at 4°C for 10 min, and the absorbance of the 100-fold diluted plasma was measured. The vascular permeability index was defined as the ratio of the tissue and plasma concentrations of Evans blue: (tissue Evans blue concentration/plasma Evans blue concentration) * 100.

SMA blood flow. The SMA flow signals (T206 Animal Research Flowmeter; Transonic Systems Inc, Ithaca, NY) were measured continuously and recorded with a computerized data acquisition system (Experimetria Ltd, Budapest, Hungary).

Intravital videomicroscopy of the ileal microcirculation. A technique of intravital, orthogonal polarization spectral imaging (Cytoscan A/R, Cytometrics, Philadelphia, PA) was used for the visualization of the serosal and mucosal microcirculation of the ileum. This technique uses reflected polarized light at the wavelength of the isosbestic point of oxyhemoglobin and deoxyhemoglobin (548 nm). Because polarization is preserved in reflection, only photons scattered from a depth of 200 mm contribute to image formation.

A 10x objective was placed onto the serosal surface of the ileum, and microscopic images were recorded with an S-VHS video recorder (Panasonic AG-TL 700, Matsushita Electric Ind Co Ltd, Osaka, Japan). The quantitative assessment of the microcirculatory parameters was performed off-line by a frame-to frame blinded analysis of the videotaped images. Changes in red blood cell (RBC) velocity (mm/s) in the postcapillary venules were determined in 3 separate fields by means of a computer-assisted image analysis system (IVM Pictron, Budapest, Hungary). All microcirculatory evaluations were performed by the same investigator (E. T.).

In vivo histology. The extent of superficial epithelial damage of the terminal ileum was evaluated by means of fluorescence confocal laser scanning endomicroscopy (CLSEM) (Five1 Optiscan Pty Ltd, Melbourne, Victoria, Australia) developed for in vivo histology. The mucosal surface of the terminal ileum 10 cm proximal to the cecum was exposed operatively and laid flat for examination. The injury of the mucosal architecture was examined after topical application of the fluorescent dye acriflavin. The surplus dye was washed off with 154 mM NaCl; then the objective of the device was placed onto the mucosal surface of the ileum and confocal imaging was performed 2 min after dye administration (1 scan per image, 1024 × 1024 pixels and 475 × 475 mm per image).

Nonoverlapping fields were processed and evaluated by a modified semiquantitative scoring system.[28] The grading was performed using the 5 following criteria: Criterion I, denudation of villi (0 = no denudation, 1 = at least one denuded area per field of view, 2 = more than one area without any recognizable villus structure per field of view; Criterion II, edema (0 = no edema, 1 = moderate epithelial swelling, 2 = severe edema); Criterion III, shedding (0 = normal, clearly, well-defined villus structure without shedding cells, 1 = some shedding cells; fewer than 30 cells per field of view, 2 = shedding cells, more than 30 cells per field of view, 3 = severe debris); Criterion IV, epithelial gap (0 = no gap, 1 = less than 5 gaps per villi, 2 = more than 5 gaps per villi); and Criterion V, longitudinal fissure on villi (0 = no fissure, 1 = presence of fissure). A blinded analysis of the same images was performed twice off-line (A.T.M.).

Preparation of ileum biopsies. Ileum biopsies kept on ice were homogenized in a phosphate buffer (pH 7.4) containing Tris-HCl (50 mM, Reanal, Budapest, Hungary), EDTA (0.1 mM), dithiotreitol (0.5 mM), phenylmethylsulfonyl fluoride (1 mM), soybean trypsin inhibitor (10 μg/mL), and leupeptin (10 μg/mL). The homogenate was centrifuged at 4°C for 20 min at 24,000*g* (Amicon Centricon-100; Millipore Corporation, Bedford, MA). Tissue concentration of nitrotyrosine (NTyr) was determined in the supernatant, while myeloperoxidase (MPO) activity was measured in the pellet of the homogenate.

Tissue MPO activity. The activity of MPO as a marker of tissue leukocyte infiltration was measured in the pellet of the homogenate using the modified method of Kuebler et al.[29] In brief, the pellet was resuspended in a K_3PO_4 buffer (0.05 M; pH 6.0) containing 0.5 % hexa-1,6-bis-decyltriethylammonium bromide. After 3 repeated freeze-thaw procedures, the material was centrifuged at 24,000*g* at 4°C for 20 min with the supernatant used for MPO determination. Afterward, 0.15 mL of 3,3′,5,5′-tetramethylbenzidine (dissolved in DMSO; 1.6 mM) and 0.75 mL of hydrogen peroxide (dissolved in K_3PO_4 buffer; 0.6 mM) were added to 0.1 mL of the sample. The reaction led to the hydrogen peroxide–dependent oxidation of tetramethylbenzidine, which was detected spectrophotometrically at 450 nm (UV-1601 spectrophotometer; Shimadzu Corp). MPO activities were measured at 37°C; then the reaction was stopped after 5 min by the addition of 0.2 mL of H_2SO_4 (2 M), and the resulting data were normalized to the protein content.

Tissue levels of NTyr. Free NTyr as a marker of peroxynitrite (ONOO) generation was measured by an enzyme-linked, immunosorbent assay (Cayman Chemical, Ann Arbor, MI). Small intestinal tissue samples were homogenized and centrifuged at 24,000*g*. The supernatants were collected and incubated overnight with anti-NTyr rabbit IgG and an NTyr acetylcholinesterase tracer in precoated (mouse anti-rabbit IgG) microplates, which were developed using Ellman's reagent. The NTyr content was normalized to the protein content of the small intestinal homogenate and expressed in ng/mg.

Plasma endothelin-1 (ET-1) levels. Blood samples (0.5 mL) were taken from the inferior caval vein into chilled polypropylene tubes containing EDTA (1 mg/mL) in the final stage of the "late reperfusion" experiments (180 min after reperfusion), centrifuged at 1,000*g* at 4°C for 30 min, and then stored at −70°C until assay. The plasma ET-1 concentration was determined in duplicates by means of a commercially available, enzyme-linked, immunosorbent assay kit (Biochemica Hungaria Ltd, Budapest, Hungary) and expressed as fmol/mL.

Intestinal superoxide ($O_2^{\bullet -}$) production. The rate of $O_2^{\bullet -}$ production in freshly minced intestinal biopsy samples was assessed using the lucigenin-enhanced chemiluminescence assay

described by Ferdinandy et al.[30] In short, approximately 10 mg of intestinal tissue was placed in 1 mL of Dulbecco's solution (pH 7.4) containing 5 μM of lucigenin. The manipulations were performed without external light 2 min after dark adaptation. Chemiluminescence was measured at room temperature in a liquid scintillation counter using a single active photomultiplier positioned in out-of-coincidence mode in the presence or absence of the $O_2^{\bullet -}$ scavenger nitroblue tetrazolium (NBT; 20 μl). NBT-inhibited chemiluminescence was interpreted as an indicator of intestinal $O_2^{\bullet -}$ generation.

Tissue and blood CH_4 levels. The CH_4 concentration in tissue was measured by means of photoacoustic spectroscopy, as reported earlier.[31] The device had been calibrated previously with various gas mixtures prepared by dilution of 1 vol% of CH_4 in synthetic air; this device has a dynamic range of 4 orders of magnitude; the minimum online detectable concentration of the sensor was found to be 0.25 ppm (3σ), with an integration time of 12 s.[31]

In a separate set of experiments, tissue CH_4 concentration was measured multiple times in anesthetized rats after inhalation of room air or artificial air containing 2.2% exogenous CH_4. At given timepoints (see Fig 2 for details), a 200 mg ileum sample was taken, excess fluid was wiped immediately off, and the tissue specimen was placed in a glass vial with 20 mL headspace volume and closed so as to be airtight. Parallel to taking ileum biopsies, 1 mL of blood was taken from the common carotid artery of the same animals through a silicone cannula and was transferred subsequently to identical glass vials. The outlet of the vials was connected to the pump of the spectroscope and headspace gas was pumped into the chamber of the device with a rate of 10 mL/min.

Photoacoustic spectroscopy is a special type of spectroscopy that measures optical absorption indirectly via the conversion of absorbed light energy into acoustic waves. The amplitude of the generated sound is directly proportional to the concentration of the absorbing gas component. The light source of the system is a near-infrared diode laser that emits light around the absorption line of CH_4 at 1650.9 nm with an output power of 15 mW (NTT Electronics, Tokyo, Japan). The cross-sensitivity for common components of breath and ambient air were examined repeatedly, and no measurable instrument response was found for several vol% of CO_2 or H_2O vapor. The narrow line width of the diode laser provides high selectivity; the absorbance of CH_4 is several orders of magnitude greater than that of H_2O, CO_2, or CO at 1.65 μm which was the wavelength we used. The CH_4 values were corrected for background levels and expressed in parts per million (ppm).

In vitro microrheologic study. *Study design, induction of oxidative stress, and CH_4 treatment.* Venous blood from healthy male volunteers was collected in lithium heparin-coated tubes. Blood samples were placed into 3 groups and incubated for 120 min at 37°C on a roller bed before performing measurements of RBC aggregation and deformability. A nontreated sample served as the negative control. Oxidative stress was induced with the addition of phenazine methosulfate (PMS, dissolved in phosphate-buffered saline, final concentration 200 μM) and incubation for 120 min.[32]

Before the study, a dose-response experiment was performed with PMS concentrations between 0 and 400 μM to determine the effective concentration. In the third, CH_4-treated group, the headspace of the sample was perfused continuously with a gas mixture containing 2.2 % CH_4 in normoxic air (Messer Hungarogaz, Budapest, Hungary) for 10 min after the end of the PMS incubation protocol. RBC deformability and the aggregation of samples were determined by means of ektacytometry and light-transmission aggregometry immediately after the incubation period. Samples here were taken from the same vials for both measurements.

RBC deformability. RBC deformability in response to shear forces was determined via a LORCA ektacytometer (Laser-assisted Optical Rotational Cell Analyzer; R&R Mechatronics, Hoorn, The Netherlands). Immediately after the treatment protocol, 20 μL of blood was suspended in 4 mL of a polyvinylpyrrolidon solution, with a viscosity of 29.8 mPas, and injected into the cylinder of the ektacytometer. During the measurement, the temperature was kept at 37°C. Deformation is characterized by the elongation index (EI) calculated from the diffraction pattern of laser light on elongated RBCs. The light was captured and analyzed by a video camera and a computer system that calculated an EI as the (length − width)/(length + width) of the pattern for 9 different shear stress values ranging from 0.5 Pa to 50 Pa.[33]

RBC aggregation. The aggregation characteristics of erythrocytes were assessed using a light transmission method described previously.[34] Immediately after the treatment protocol, 30 μL of blood was transferred to a Myrenne MA-1 Aggregometer (Myrenne GmbH, Roetgen, Germany). The blood sample was first sheared at 600 s^{-1} to disperse all pre-existing aggregates,

then the shear rate decreased rapidly to low shear rates. The extent of aggregation was characterized by the aggregation index, calculated using the surface area below the light intensity curve in a 10 s period. Measurements were performed at ambient room temperature.

Statistical analysis. GraphPad Prism 5.01 for Windows (GraphPad Software, La Jolla, CA) was used for a statistical evaluation of the data. The statistical analysis was performed by a 2-way analysis of variance of repeated measures followed by Bonferroni post hoc test in normally distributed data and a Kruskal-Wallis 1-way analysis of variance on ranks combined with the Dunn method for pairwise multiple comparisons in groups showing a non-Gaussian distribution. Taking into account the fact that parts of the in vivo data were not normally distributed (not Gaussian), we displayed the data as box plots where possible. Median values and the interquartile ranges of the 75th and 25th percentiles are given.

RESULTS

Inhaled CH_4 is transported by the blood and the gas accumulates in intestinal tissue. The CH_4 concentration in the baseline samples of non-CH_4-producer animals remained below the background levels in both the arterial blood and in the ileal tissue prior to the beginning of the experiment (Fig 2, *A* and *B*, "Baseline"). After 5 min of normoxic CH_4 inhalation with a flow rate of 300 mL/min, at the end of the SMA ischemia, substantially increased concentrations of CH_4 were detected in the systemic arterial blood and a slight increase in the ileum as well (Fig 2, *A* and *B*, "Isch 45′–CH_4 5′"). At 10 min into the reperfusion phase, at the end of the 15 min inhalation of normoxic CH_4-air mixture, CH_4 concentration in the ileal tissue also increased (Fig 2, *B*, "Rep 10′–CH_4 15′"). In samples taken at the 60th min of the reperfusion, 50 min after the end of CH_4 treatment, no significant amounts of CH_4 were found in intestinal or blood samples (Fig 2, *A* and *B*, "Rep 60").

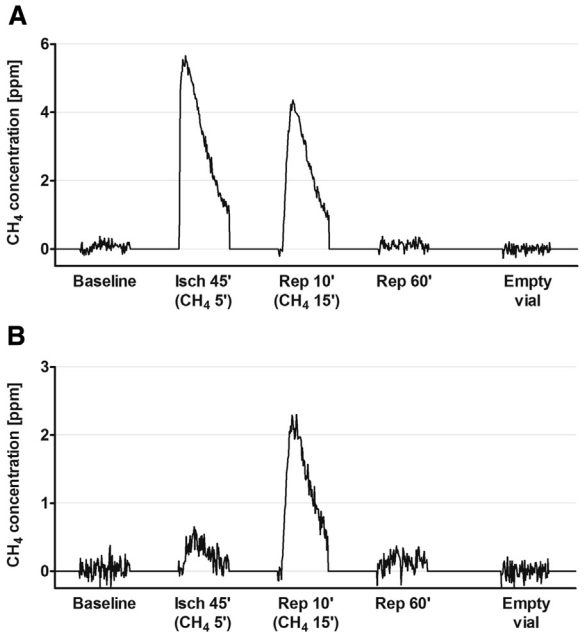

Fig 2. CH_4 concentrations in blood (*A*) and ileum (*B*) samples taken during the CH_4-air inhalation protocol in a pilot study. Original recording of photoacoustic signals as a function of time. At the indicated time point during the experiments, a tissue sample of the ileum, weighing approximately 200 mg was taken and placed immediately in a glass vial. Simultaneously, blood samples (1 mL each) were taken from the common carotid artery into glass vials. Gas samples from the headspace (20 mL) were transferred to the photoacoustic detection system, and each tissue specimen was measured for 10 min. Values are expressed as parts per million (ppm) and are corrected for background CH_4 levels. Baseline—prior to CH_4 inhalation and ischemia. Isch 45′ (CH_4 5′)—end of mesenteric ischemia, 5 min of normoxic CH_4 inhalation. Rep 10' (CH_4 15′) —tenth min of reperfusion, end of the 15-min normoxic CH_4 inhalation. Rep 60′—60th min of reperfusion. Empty vial—CH_4 concentration without biological sample, used for background correction.

The small intestinal epithelial barrier function. Epithelial permeability (EP) and vascular permeability (VP) indices were determined simultaneously to assess the barrier function of the intestinal mucosa during the re-establishment of the blood flow to the previously ischemic tissues (Fig 3, *A*). The EP did not change in sham-operated control animals, while the plasma levels of FD4 increased steeply in the IR group, indicating a rapid deterioration of the epithelial barrier function. Normoxic CH_4 treatment resulted in significantly lesser EP levels, implying preserved interepithelial junctions.

Later in the reperfusion phase (Fig 3, *B*), the EP index in nontreated animals decreased, suggesting an improved barrier function compared to that in the early phase; while in the CH_4-treated group, the change was similar to that observed in the early phase of reperfusion. The EP index remained at the baseline level in the control animals.

Small intestinal microvascular barrier function. No statistically significant changes in the VP assessed by Evans blue extravasation were detected

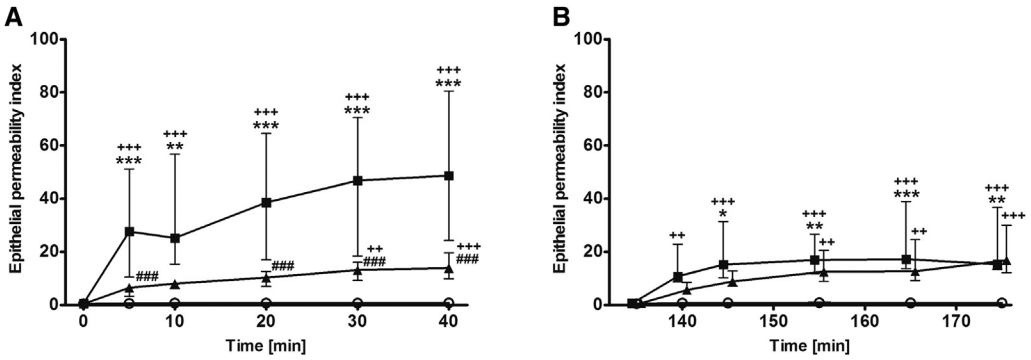

Fig 3. Changes in epithelial permeability (EP) in the sham-operated (*empty circles*), mesenteric IR (*black squares*), and CH_4-treated IR (*black triangles*) groups during early (*A*) and late phases (*B*) of reperfusion. The EP was assessed in each period, and the permeability index was calculated as described earlier (see the Methods section for a description of the experiments). Data are expressed as median, 25th, and 75th percentiles. Here, * means $P < .05$; ** means $P < .01$ and *** means $P < .001$ between groups versus sham-operated group; ### means $P < .001$ between CH_4-treated and IR groups, while ++ means $P < .01$ and +++ $P < .001$ compared to baseline values within groups.

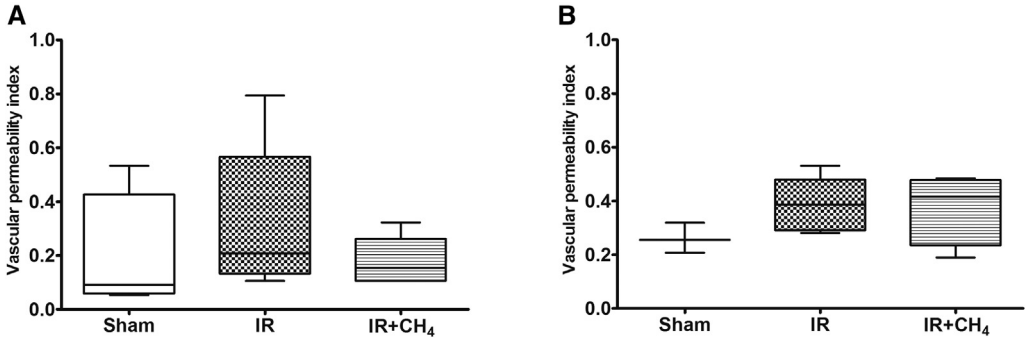

Fig 4. Changes in vascular permeability (VP) in the sham-operated (Sham, *empty boxes*), mesenteric IR (IR, *checkered boxes*), and CH_4-treated IR (IR+CH_4, *hatched boxes*) groups during early (*A*) and late phases (*B*) of reperfusion. The VP index was calculated using a spectrophotometric evaluation of Evans Blue extravasation (see Materials and Methods section). The results are expressed as median, 25th, and 75th percentiles.

either in the early (Fig 4, *A*) or the later phases (Fig 4, *B*) of reperfusion.

Macro- and microcirculatory changes. The SMA blood flow was assessed continuously during the experiments (Fig 5). In the IR and IR + CH_4 groups, the complete cessation of blood flow was followed by different reactions during reperfusion. The SMA flow in the IR group remained significantly low as compared to baseline levels, while in CH_4-treated animals, the SMA flow was significantly greater compared to that in the IR group.

Prior to the induction of SMA occlusion, the RBC velocity in the microvessels of the ileal serosa was similar in all groups (Fig 6). In the 15th min of reperfusion, the intestinal microcirculation of the IR group was significantly impaired. In the IR + CH_4-treated groups, the RBC velocity did not differ from that of the sham-operated groups, implying improved microcirculation. By the 120 min of the reperfusion, no differences were seen among the groups.

Tissue ET-1 levels. The ET-1 concentration was measured from plasma samples at the end of the 180-min reperfusion periods. In the IR group, there was a significant increase in ET-1 concentration at 180 min after reperfusion relative to that in the control animals. This increase was significantly decreased in the IR + CH_4-treated group (Fig 7, *A*).

Tissue MPO levels. The activity of MPO, a marker enzyme of PMN granulocytes, was assessed in intestinal homogenates at the end of the late reperfusion phase. A significant MPO elevation was present in both the IR and the CH_4-treated groups, indicating acute inflammation and extravasation of leukocytes into the tissue (Fig 7, *B*).

ROS and RNS levels. Tissue NTyr concentration (Fig 8, *A*) is an indicator of protein nitration produced by a chemical reaction associated with

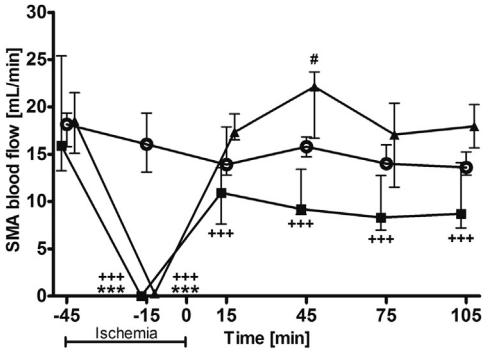

Fig 5. Changes in the superior mesenteric artery (SMA) blood flow in the sham-operated (*empty circles*), mesenteric IR (*black squares*), and CH_4-treated IR (*black triangles*) groups. 0 min on the X-axis denotes the start of reperfusion. Results are expressed as median, 25th, and 75th percentiles. Here, *** means $P < .001$ between groups versus sham-operated group; # indicates $P < .05$ between CH_4-treated and IR groups, while +++ means $P < .001$ compared with baseline values within groups.

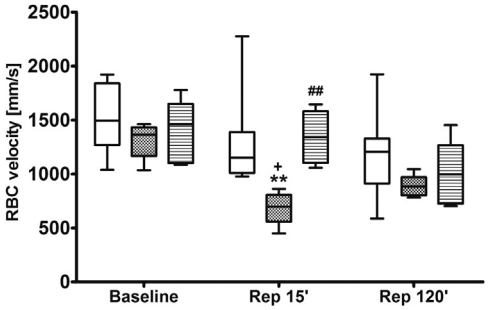

Fig 6. Changes in red blood cell (RBC) velocity in the microvessels of the serosal surface of the ileum in response to a sham operation (*empty boxes*) or 45 min of mesenteric ischemia followed by 120 min of reperfusion (IR groups, *checkered boxes*) and in rats treated with a normoxic (21% O_2) gas mixture containing 2.2% CH_4 for 5 min at the end of the ischemia and for 10 min at the beginning of the reperfusion period (IR + CH_4, *hatched boxes*). Measurements were performed at baseline conditions (Baseline), 15 min after reperfusion (Rep 15′), and 120 min after reperfusion (Rep 120′). ** means $P < .01$ between groups versus sham-operated group, ## means $P < .01$ between IR and IR + CH_4 groups, + means $P < .05$ compared with baseline values within groups.

ONOO generation. The NTyr levels were increased by the 180 min of reperfusion in the IR group as compared to those in the sham-operated controls, but the NTyr levels in the CH_4-treated group did not differ from the controls.

$O_2^{\bullet-}$ levels. A primary cellular ROS, $O_2^{\bullet-}$, was detected in ileal biopsies at the beginning of experiments (Fig 8, *B*), and no between-group differences were demonstrated. At 15 min after the reestablishment of blood flow, the samples taken from the IR group contained significantly greater levels of $O_2^{\bullet-}$ than those from the control and CH_4-treated animals.

Structural integrity of small intestinal mucosa. Intravital CLSEM images were recorded to obtain information on the structural condition of the mucosa, and these microscopic histology data were evaluated using a semiquantitative scoring system (Fig 9, *D*). Normal villi with intact epithelial cells were observed in the control group (Fig 9, *A*). When compared to the typically continuous, unbroken epithelial lining in the sham-operated animals, after 30 min of reperfusion, the mucosa was severely damaged with epithelial defects stretching across the villi seen regularly in association with increased luminal debris formation (Fig 9, *B*). No epithelial disruptions on the lumen surface were present in the CH_4-treated group (Fig 9, *C*), and the microstructural damage reflected in the injury score was significantly less than that in nontreated IR animals.

The effects of CH_4 on the microhemorheologic parameters of whole blood. The deformability of erythrocytes taken from human blood was measured using a laser-assisted, optical rotational method (Fig 10). Oxidative stress induced by in vitro treatment with the oxidizer PMS resulted in a significantly decreased elongation index from low to moderately high shear stress rates compared to that for the nontreated control samples. Normoxic CH_4 incubation applied after the oxidizer incubation was able to counteract in part the decreased rigidity of RBCs at moderate levels of shear stress (Fig 10, *A–C*). Moreover, oxidative stress in vitro increased the aggregation of erythrocytes at low shear stress compared to that in control samples (Fig 11). After applying CH_4, these values significantly decreased to the level of nontreated control samples.

DISCUSSION

Herein, we present new data on the biologic effects of normoxic CH_4 ventilation in a standardized rat model of mesenteric IR. It is well recognized that intestinal IR induces a range of humoral and cellular reactions that have a common end point in transmucosal damage.[35] The potentially destructive pathways increase the leakage of plasma into the interstitium and, conversely, luminal substances can get into the lymphatics and the bloodstream.

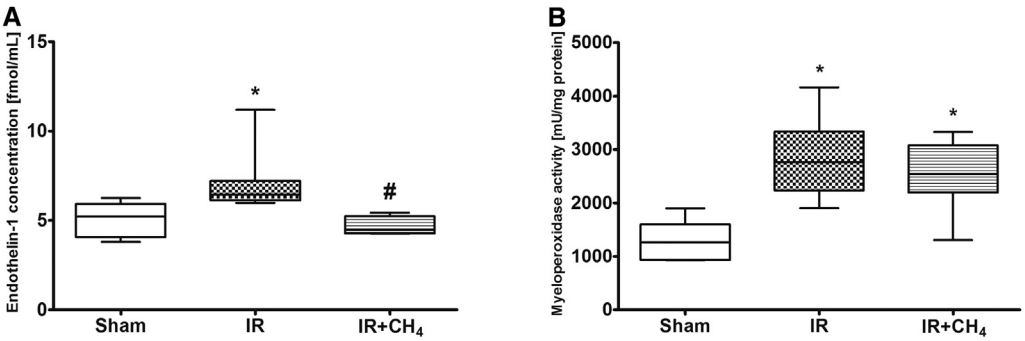

Fig 7. Changes in the plasma endothelin-1 (ET-1) concentration and tissue myeloperoxidase (MPO) activity at the end of 180 min reperfusion in the sham-operated (Sham, *empty box*), IR (*checkered box*), and CH_4-treated groups (IR + CH_4, *hatched boxes*). * means $P < .05$ between groups versus sham-operated group, # means $P < .05$ between IR and IR + CH_4 groups.

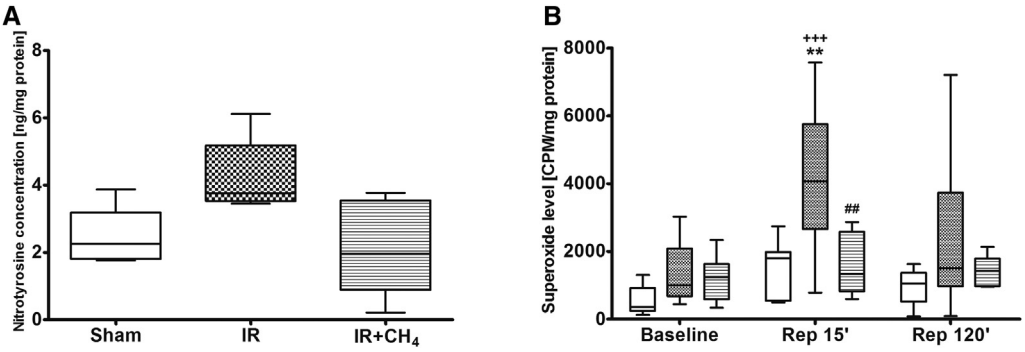

Fig 8. Changes in mucosal nitrotyrosine (panel *A*) and superoxide (panel *B*) production in sham-operated control animals (Sham, *empty boxes*) and after 45 min of SMA occlusion and 180 min reperfusion (IR group, *checkered boxes*). In the methane-treated group (IR + CH_4, *hatched boxes*), the animals inhaled a normoxic (21% O_2) gas mixture containing 2.2% CH_4 for 5 min at the end of the ischemia and for 10 min at the beginning of the reperfusion period (or 15 min in total). The nitrotyrosine level was measured by means of enzyme-linked, immunosorbent assay from samples taken after 180 min of reperfusion and normalized to the total protein content of the tissue. Superoxide levels (panel *B*) were measured by chemiluminescence at the beginning of the experiment (Baseline) and at 15 min (Rep 15′) and 120 min after reperfusion (Rep 120′), and they were normalized to the protein content of the tissue sample. Data are expressed as median, 25th, and 75th percentiles. ** means $P < .01$ compared to sham-operated group; ## means $P < .01$ between the CH_4-treated group and IR group, while +++ means $P < .001$ compared to baseline values within groups.

Although the changes in mucosal permeability can range from moderate malfunction of the tight junctions of the villus epithelium to manifest discontinuity, the preservation or restoration of the barrier is of vital importance in the salvage therapies of several acute and chronic GI diseases.[36] Our study demonstrated that normoxic CH_4 inhalation influences effectively the epithelial component of transmucosal permeability and the early structural loss of the epithelial layer.

In the present study, the early and later consequences of IR were characterized by biochemical, macro- and microcirculatory, and morphologic parameters. The IR-induced structural damage was confirmed by in vivo endomicroscopy, and direct intravital data were also obtained for the derangement of the intestinal microcirculation. The impairment of nutritive perfusion and attachment of circulating PMN leukocytes to the endothelial wall are key events in the development of IR injuries. The capillary no-reflow phenomenon[37] and the spatial microcirculatory heterogeneity can result in sustained local hypoxia. Consequently, soluble inflammatory mediators are released and, among others, ROS and RNS are produced. ET-1, the most potent vasoconstrictor, also contributes to PMN adhesion in submucosal postcapillary venules and to the detrimental microvascular consequences of mesenteric ischemia.[38] These components of the IR pathology all lead to the breakdown of membrane fences and to a critical second-wave inflammatory response.[39]

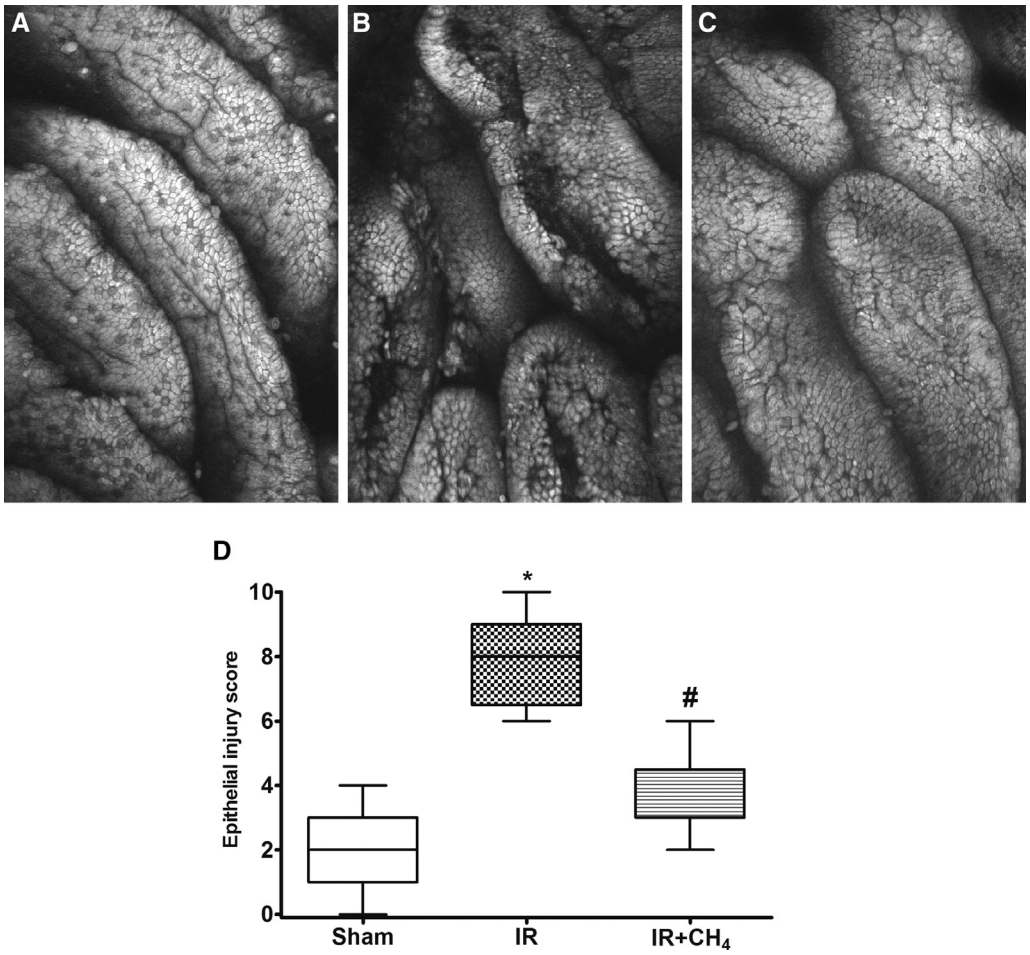

Fig 9. Top panel: in vivo histologic images recorded by confocal laser scanning endomicroscopy (CLSEM) after the topical administration of sodium acriflavine. (*A*) The normal structure of the mucosa in the control group. (*B*) Loss of epithelium with disruptions on the villus surface after 45 min SMA occlusion and 30 min reperfusion. (*C*) Nearly intact villus surface after the inhalation of a normoxic (21% O_2) gas mixture containing 2.2% CH_4 for 5 min at the end of ischemia and for 10 min at the beginning of the reperfusion period. Bottom panel (*D*): grading of in vivo histology on a semiquantitative scoring system. The plots show the median and the 25th and 75th percentiles. Here, * means $P < .05$ between groups versus sham-operated group, # means $P < .05$ between the IR and IR + CH_4 group.

There is now ample evidence that exogenous CH_4 can protect the tissues from the development of these anti-inflammatory activities. It has been shown repeatedly by various research groups that experimental CH_4 treatment counteracts inflammatory cytokine production and stimulates antioxidative defense systems.[12-16] In the current experiments, the decrease in epithelial permeability after CH_4 inhalation was associated with decreased generation of ROS and RNS and decreased ET-1 levels.

CH_4 treatment improved both serosal microcirculation and SMA flow which, in turn, delivers more oxygen to the cells and allows effective oxidative phosphorylation by mitochondria. The normalized ET-1 plasma levels in the CH_4-treated groups can reflect the improved local microcirculatory state on the one hand, and the decrease in inflammatory activation on the other. This observation accords with an earlier finding that CH_4 treatment decreases xanthine oxidoreductase activity[11]; being the most important ROS-producing enzyme in the postischemic gut,[40] the inhibition of xanthine oxidoreductase contributes to the decrease in $O_2^{\bullet -}$ production in the postischemic intestinal tissue.

In our study, we used FITC-labeled dextrane with a molecular weight of 4 kDa, a good indicator of the paracellular epithelial permeability pathway[41] mediated predominantly by tight junctions. The influence of an increased intraluminal CH_4 concentration on the epithelial permeability is of interest,

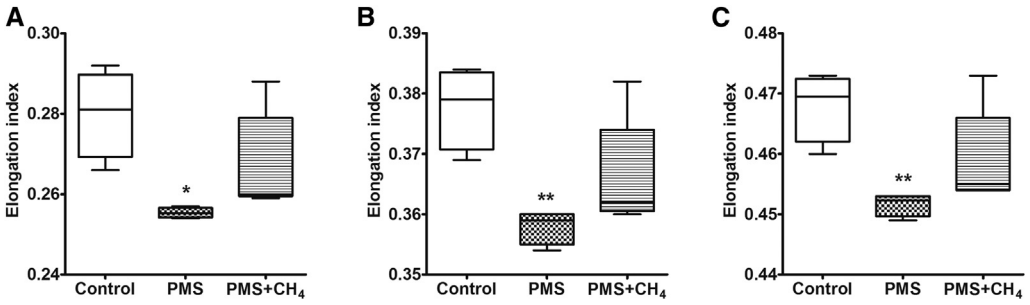

Fig 10. Changes in deformability of RBCs in vitro under increasing shear stress rates at 1.57 Pa (*A*), 2.81 Pa (*B*), and 5.00 Pa (*C*) depicted as box plots. The greater elongation indices represent more elongated, hence more oval, erythrocytes. Control samples (*empty boxes*), samples incubated with PMS for 2 h to induce oxidative stress (PMS groups, *checkered boxes*), and blood samples treated with a normoxic (21% O_2) gas mixture containing 2.2% CH_4 for 10 min after 2 h of PMS challenge (PMS + CH_4, *hatched boxes*). The box plots show the median and the 25th and 75th percentiles. Here, $*P < .05$ and $**P < .01$ PMS versus control group and $n = 4–5$.

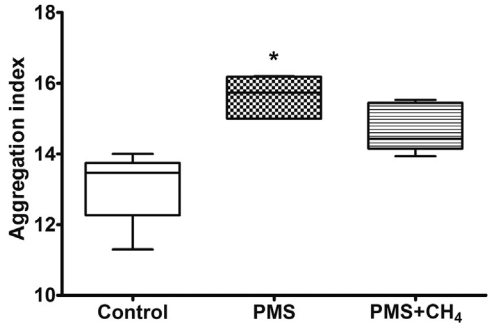

Fig 11. RBC aggregation in vitro. The light transmission of rapidly aggregating samples at low shear rates was measured for 10 s, and the aggregation index was calculated. Control samples (*empty boxes*), samples incubated with PMS for 2 h to induce oxidative stress (PMS group, *checkered boxes*), and blood samples treated with a normoxic (21% O_2) gas mixture containing 2.2% CH_4 for 10 min after 2 h of PMS challenge (PMS + CH_4, *hatched boxes*). The plots show the median and the 25th and 75th percentiles. Here, * means $P < .05$ PMS versus control group and $n = 4–5$.

especially when we recall the importance of maintaining the intestinal barrier in many clinical settings.[42] In theory, CH_4 can protect tight junctions from opening by directly influencing membrane fluidity or by preserving the ATP levels of epithelial cells. The maintenance of intercellular tight junctions among mucosal epithelial cells is an energy-dependent mechanism.[43] The improved micro- and macrocirculation of the postischemic gut after CH_4 treatment was demonstrated in the present study; hence, increased oxidative phosphorylation early in the reperfusion may allow the cells to return to sufficient energy levels that maintain tight junction proteins in the tightly closed conformation.

Because no specific receptors or other signalling molecules of CH_4 have been reported to date, we hypothesized that CH_4 can modulate plasma membrane fluidity by being dissolved in the apolar lipid phase. The tissue NTyr level is an indicator of protein nitration, associated with increased levels of peroxynitrite, which is a potent initiator of membrane lipid peroxidation[44]; it was reported earlier that IR-associated lipid peroxidation decreases membrane fluidity in various tissues[45] and in erythrocytes as well.[46] The membrane and cytoskeleton are responsible together for altering the shape of the erythrocyte.[47] Lipid peroxidation breaks the connection between the 2 components,[48] and consequently, both the deformability and aggregation of the RBCs is influenced in a detrimental way.[49] Brath et al[50] reported worsened RBC deformability and increased aggregation in the early reperfusion after experimental mesenteric ischemia in the rat portal vein. Because normal erythrocytes are approximately 25% greater in diameter than the mean diameter of capillaries, sufficient RBC deformability is a prerequisite in normal capillary blood flow.[51,52]

With this in mind, an in vitro microrheologic study with human whole blood was designed without the confounding in vivo effects of vasoactive metabolites. We showed that an oxidative challenge significantly decreased the elongation index of RBCs. With normoxic CH_4 treatment, the RBC deformability improved at low to moderate shear stress rates, suggesting a direct effect of CH_4 on membrane fluidity and/or membrane-cytoskeleton junctions. Aggregation was measured in the same experimental setting at low rates of shear stress. Once again, the increased aggregation index of RBCs provided evidence for the role of

oxidative stress in our setup, and CH_4 treatment alleviated this response.

Thus, these data provide evidence for the direct, beneficial effects of CH_4 exerted in the oxidized biomembranes of erythrocytes. The improvement in microcirculation with CH_4 treatment is probably the net result of a complex mechanism, with decreased production of $O_2^{\bullet -}$ and less membrane damage (indicated by lesser levels of malondialdehyde, reported previously[21]) while, at the same time, accumulation of CH_4 in the lipid phase further increases RBC deformability.

The effects of CH_4 on the IR-induced changes in vascular permeability are less clear, because in this model, the epithelial and endothelial permeability-specific changes were affected differentially by the IR cycle. Epithelial permeability significantly deteriorated immediately after reperfusion, while the extravasation of the circulating endothelial tracer did not increase to a great extent. Therefore, the relative effect of CH_4 administration on microvascular permeability could not be evaluated simultaneously. We assume that CH_4 diffused from the circulating blood through the endothelial layer, a step which should lead to a continuous CH_4 supply to the endothelial cell membranes as well; however, we cannot exclude a possible interference of the techniques (ie, FITC-labeled dextrane and Evans blue measurements). The measurements of epithelial and endothelial permeability were conducted simultaneously in the same animal for ethical reasons, and this approach could influence the sensitivity of these methods. Therefore, future studies are needed to examine the influence of CH_4 on microvascular permeability directly and independent of other factors.

An assessment of the kinetics of the inhaled CH_4 revealed that in our inhalation regimen, significant amounts of CH_4 are already in the systemic circulation at the end of reperfusion, allowing rapid equilibration with the intestinal tissue early in the reperfusion, as confirmed by photoacoustic spectroscopy measurements. By the 60th min of reperfusion, CH_4 levels fell to the baseline levels.

The effects of CH_4 inhalation were studied for 60 min and 180 min after the restoration of the mesenteric blood flow. The epithelial barrier of the ileum was already restored in part in the later phase of the reperfusion, as indicated by the lesser FD4 clearances, both in the IR and IR + CH_4-treated groups. The normalizing signs seen after the transient ischemic challenge support our assumption that the intestinal metabolism was returning to normal.

The difference between the intensities of early and later changes in epithelial permeability, however, suggest that on the re-establishment of the blood and oxygen supply, the endogenous defense mechanisms cannot immediately control or counteract the damaging reactions. Salvage therapies should target this initial step to avoid long-term or distant consequences of the barrier damage, and CH_4 treatment met this need. Although even a brief 15-min CH_4 inhalation preserved the function of the postischemic gut sufficiently, continuous, long-term CH_4 supplementation might have additional beneficial effects.

In conclusion, our results revealed that IR leads to significant increases in epithelial permeability, and CH_4 is able to counteract these detrimental effects at this early and decisive phase of the loss of mucosal integrity; however, it is still not known whether the findings in this experimental model are applicable in other conditions. It remains to be determined what role the transmembrane proteins of the epithelial tight junctions play into this effect and through what steps CH_4 is able to modulate the intercellular connections.

We demonstrated that CH_4 improves directly the deformability and aggregation of erythrocytes on oxidative stress. Moreover, we provide here the first detailed measurements of the distribution kinetics of inhaled CH_4 in an animal model of mesenteric IR. One limitation of the study, however, is that we did not assess directly the conformational changes of tight junction proteins, which was beyond the scope of the present study. To address these issues, further investigations are needed, but the data presented here establish clearly a mucosa-protective, antipermeability role for exogenous CH_4 administration.

The authors are grateful to Ms Csilla Mester, Mrs Nikolett Beretka, and Mrs Lilla Ágnes Szilágyi for their skillful assistance during the in vivo experiments. The microhemorheological study was performed at the First Department of Medicine, University of Pécs, Hungary, and the generous help of Prof Kálmán Tóth, Dr Gábor Késmárky, Dr Péter Rábai, Dr András Tóth, Dr Barbara Sándor, and Dr István Juricskay was greatly appreciated.

REFERENCES

1. Mallick IH, Yang W, Winslet MC, Seifalian AM. Ischemia-reperfusion injury of the intestine and protective strategies against injury. Dig Dis Sci 2004;49:1359-77.
2. Fink MP. Intestinal epithelial hyperpermeability: update on the pathogenesis of gut mucosal barrier dysfunction in critical illness. Curr Opin Crit Care 2003;9:143-51.

3. Schlichtig R, Bowles SA. Distinguishing between aerobic and anaerobic appearance of dissolved CO_2 in intestine during low flow. J Appl Physiol 1994;76:2443-51.
4. Buchholz BM, Kaczorowski DJ, Sugimoto R, Yang R, Wang Y, Billiar TR, et al. Hydrogen inhalation ameliorates oxidative stress in transplantation induced intestinal graft injury. Am J Transplant 2008;8:2015-24.
5. Vince AJ, Burridge SM. Ammonia production by intestinal bacteria: the effects of lactose, lactulose and glucose. J Med Microbiol 1980;13:177-91.
6. Vandiver M, Snyder SH. Hydrogen sulfide: a gasotransmitter of clinical relevance. J Mol Med (Berl) 2012;90:255-63.
7. Romagnuolo J, Schiller D, Bailey RJ. Using breath tests wisely in a gastroenterology practice: an evidence-based review of indications and pitfalls in interpretation. Am J Gastroenterol 2002;97:1113-26.
8. Keppler F, Hamilton JT, Brass M, Rockmann T. Methane emissions from terrestrial plants under aerobic conditions. Nature 2006;439:187-91.
9. Tuboly E, Szabo A, Garab D, Bartha G, Janovszky A, Eros G, et al. Methane biogenesis during sodium azide-induced chemical hypoxia in rats. Am J Physiol Cell Physiol 2013;304:C207-14.
10. Triantafyllou K, Chang C, Pimentel M. Methanogens, methane and gastrointestinal motility. J Neurogastroenterol Motil 2014;20:31-40.
11. Boros M, Ghyczy M, Erces D, Varga G, Tokes T, Kupai K, et al. The anti-inflammatory effects of methane. Crit Care Med 2012;40:1269-78.
12. Fan DF, Hu HJ, Sun Q, Lv Y, Ye ZH, Sun XJ, et al. Neuroprotective effects of exogenous methane in a rat model of acute carbon monoxide poisoning. Brain Res 2016;1633:62-72.
13. Liu L, Sun Q, Wang R, Chen Z, Wu J, Xia F, et al. Methane attenuates retinal ischemia/reperfusion injury via antioxidative and anti-apoptotic pathways. Brain Res 2016;1646:327-33.
14. Shen M, Fan D, Zang Y, Chen Y, Zhu K, Cai Z, et al. Neuroprotective effects of methane-rich saline on experimental acute carbon monoxide toxicity. J Neurol Sci 2016;369:361-7.
15. Xin L, Sun X, Lou S. Effects of methane-rich saline on the capability of one-time exhaustive exercise in male SD rats. PLoS One 2016;11:e0150925.
16. Zhang X, Li N, Shao H, Meng Y, Wang L, Wu Q, et al. Methane limit LPS-induced NF-κB/MAPKs signal in macrophages and suppress immune response in mice by enhancing PI3K/AKT/GSK-3β-mediated IL-10 expression. Sci Rep 2016;6:29359.
17. Wu J, Wang R, Ye Z, Sun X, Chen Z, Xia F, et al. Protective effects of methane-rich saline on diabetic retinopathy via anti-inflammation in a streptozotocin-induced diabetic rat model. Biochem Biophys Res Commun 2015;466:155-61.
18. Ye Z, Chen O, Zhang R, Nakao A, Fan D, Zhang T, et al. Methane attenuates hepatic ischemia/reperfusion injury in rats through antiapoptotic, anti-inflammatory, and antioxidative actions. Shock 2015;44:181-7.
19. Chen O, Ye Z, Cao Z, Manaenko A, Ning K, Zhai X, et al. Methane attenuates myocardial ischemia injury in rats through anti-oxidative, anti-apoptotic and anti-inflammatory actions. Free Radic Biol Med 2016;90:1-11.
20. He R, Wang L, Zhu J, Fei M, Bao S, Meng Y, et al. Methane-rich saline protects against concanavalin A-induced autoimmune hepatitis in mice through anti-inflammatory and anti-oxidative pathways. Biochem Biophys Res Commun 2016;470:22-8.
21. Strifler G, Tuboly E, Szél E, Kaszonyi E, Cao C, Kaszaki J, et al. Inhaled methane limits the mitochondrial electron transport chain dysfunction during experimental liver ischemia-reperfusion injury. PLoS One 2016;11:e0146363.
22. Song K, Zhang M, Hu J, Liu Y, Liu Y, Wang Y, et al. Methane-rich saline attenuates ischemia/reperfusion injury of abdominal skin flaps in rats via regulating apoptosis level. BMC Surg 2015;15:92.
23. Wang R. Gasotransmitters: growing pains and joys. Trends Biochem Sci 2014;39:227-32.
24. Blikslager AT, Moeser AJ, Gookin JL, Jones SL, Odle J. Restoration of barrier function in injured intestinal mucosa. Physiol Rev 2007;87:545-64.
25. Cuzzocrea S, Zingarelli B, Costantino G, Szabo A, Salzman AL, Caputi AP, et al. Beneficial effects of 3-aminobenzamide, an inhibitor of poly (ADP-ribose) synthetase in a rat model of splanchnic artery occlusion and reperfusion. Br J Pharmacol 1997;121:1065-74.
26. Szentpali K, Kaszaki J, Tiszlavicz L, Lazar G, Balogh A, Boros M. Bile-induced adenosine triphosphate depletion and mucosal damage during reflux esophagitis. Scand J Gastroenterol 2001;36:459-66.
27. Lowry OH, Rosebrough NJ, Farr AL, Randall RJ. Protein measurement with the Folin phenol reagent. J Biol Chem 1951;193:265-75.
28. Érces D, Nógrády M, Varga G, Szűcs S, Mészáros AT, Fischer-Szatmári T, et al. Complement C5a inhibition improves late hemodynamic and inflammatory changes in a rat model of nonocclusive mesenteric ischemia. Surgery 2016;159:960-71.
29. Kuebler WM, Abels C, Schuerer L, Goetz AE. Measurement of neutrophil content in brain and lung tissue by a modified myeloperoxidase assay. Int J Microcirc Clin Exp 1996;16:89-97.
30. Ferdinandy P, Danial H, Ambrus I, Rothery RA, Schulz R. Peroxynitrite is a major contributor to cytokine-induced myocardial contractile failure. Circ Res 2000;87:241-7.
31. Tuboly E, Szabo A, Eros G, Mohacsi A, Szabo G, Tengolics R, et al. Determination of endogenous methane formation by photoacoustic spectroscopy. J Breath Res 2013;7:046004.
32. Rabai M, Toth A, Kenyeres P, Mark L, Marton Z, Juricskay I, et al. In vitro hemorheological effects of red wine and alcohol-free red wine extract. Clin Hemorheol Microcirc 2010;44:227-36.
33. Hardeman MR, Goedhart PT, Schut NH. Laser-assisted optical rotational cell analyser (LORCA). II: Red blood cell deformability: elongation index versus cell transit time. Clin Hemorheol Microcirc 1994;14:619-30.
34. Kiesewetter H, Radtke H, Schneider R, Mußler K, Scheffler A, Schmid-Schönbein H. [Mini erythrocyte aggregometer: a new apparatus for rapid quantification of the extent of erythrocyte aggregation]. Biomed Tech (Berl) 1982;27:209-13; German.
35. Swank GM, Deitch EA. Role of the gut in multiple organ failure: bacterial translocation and permeability changes. World J Surg 1996;20:411-7.
36. Teshima CW, Meddings JB. The measurement and clinical significance of intestinal permeability. Curr Gastroenterol Rep 2008;10:443-9.
37. Schmid-Schonbein GW. Capillary plugging by granulocytes and the no-reflow phenomenon in the microcirculation. Fed Proc 1987;46:2397-401.
38. Martinez-Revelles S, Caracuel L, Marquez-Martin A, Dantas A, Oliver E, D'Ocon P, et al. Increased endothelin-

1 vasoconstriction in mesenteric resistance arteries after superior mesenteric ischaemia-reperfusion. Br J Pharmacol 2012;165:937-50.
39. Vajda K, Szabo A, Kucsa K, Suki B, Boros M. Microcirculatory heterogeneity in the rat small intestine during compromised flow conditions. Microcirculation 2004;11:307-15.
40. Granger DN, Kvietys PR. Reperfusion injury and reactive oxygen species: the evolution of a concept. Redox Biol 2015;6:524-51.
41. Szabo A, Menger MD, Boros M. Microvascular and epithelial permeability measurements in laboratory animals. Microsurgery 2006;26:50-3.
42. Tuboly E, Mészáros A, Boros M. Nonbacterial biotic methanogenesis, possible mechanisms and significance. In: Gholikandi GB, editor. Methanogenesis: biochemistry, ecological functions, natural and engineered environments. Hauppauge (NY): Nova Science Publishers; 2014.
43. Wattanasirichaigoon S, Menconi MJ, Delude RL, Fink MP. Effect of mesenteric ischemia and reperfusion or hemorrhagic shock on intestinal mucosal permeability and ATP content in rats. Shock 1999;12:127-33.
44. Hogg N, Kalyanaraman B. Nitric oxide and lipid peroxidation. Biochim Biophys Acta 1999;1411:378-84.
45. Dobretsov GE, Borschevskaya TA, Petrov VA, Vladimirov YA. The increase of phospholipid bilayer rigidity after lipid peroxidation. FEBS Lett 1977;84:125-8.
46. Watanabe H, Kobayashi A, Yamamoto T, Suzuki S, Hayashi H, Yamazaki N. Alterations of human erythrocyte membrane fluidity by oxygen-derived free radicals and calcium. Free Radic Biol Med 1990;8:507-14.
47. Reinhart WH. Molecular biology and self-regulatory mechanisms of blood viscosity: a review. Biorheology 2001;38:203-12.
48. Mohandas N, Chasis JA. Red blood cell deformability, membrane material properties and shape: regulation by transmembrane, skeletal and cytosolic proteins and lipids. Semin Hematol 1993;30:171-92.
49. Kayar E, Mat F, Meiselman HJ, Baskurt OK. Red blood cell rheological alterations in a rat model of ischemia-reperfusion injury. Biorheology 2001;38:405-14.
50. Brath E, Nemeth N, Kiss F, Sajtos E, Hever T, Matyas L, et al. Changes of local and systemic hemorheological properties in intestinal ischemia-reperfusion injury in the rat model. Microsurgery 2010;30:321-6.
51. Reinhart WH, Chien S. Roles of cell geometry and cellular viscosity in red cell passage through narrow pores. Am J Physiol 1985;248:C473-9.
52. Baskurt OK, Meiselman HJ. Blood rheology and hemodynamics. Semin Thromb Hemost 2003;29:435-50.